LIF supports primitive endoderm expansion during pre-implantation development

Sophie M. Morgani[1] and Joshua M. Brickman[1*]

1. The Danish Stem Cell Centre - DanStem, University of Copenhagen, 3B Blegdamsvej, DK-2200 Copenhagen N

*Correspondence to Joshua.brickman@sund.ku.dk

Summary

Embryonic stem cells (ESCs) are pluripotent cell lines that can be maintained indefinitely in an early developmental state. ESC culture conditions almost all require the cytokine LIF to maintain self-renewal. As ESCs are not homogeneous, but contain multiple populations reminiscent of the blastocyst, identifying the target cells of LIF is necessary to understand the propagation of pluripotency. We recently found that LIF acts under self-renewing conditions to stimulate the fraction of ESCs that express extraembryonic markers, but has little impact on pluripotent gene expression. Here we report that LIF has two distinct roles. It blocks early epiblast differentiation and supports the expansion of primitive endoderm (PrE) primed ESCs and PrE *in vivo*. We find that activation of JAK/STAT signalling downstream of LIF occurs initially throughout the pre-implantation embryo, but later marks the PrE. Moreover, the addition of LIF to cultured embryos increases the GATA6^{+} PrE population while inhibition of JAK/STAT reduces both NANOG^{+} epiblast (Epi) and GATA6^{+} PrE. The reduction of the NANOG^{+} Epi may be explained by its precocious differentiation to later Epi derivatives, while the increase in PrE is mediated both by an increase in proliferation and inhibition of PrE apoptosis that is normally triggered in embryos with an excess of GATA6^{+} cells. Thus, it appears that the relative size of the PrE is determined by the number of LIF-producing cells in the embryo. This suggests a mechanism by which the embryo adjusts the relative ratio of the primary lineages in response to experimental manipulation.

Introduction

Embryonic stem cells (ESCs) are karyotypically normal self-renewing cell lines derived from the mammalian embryo during pre-implantation development. They are typically considered to be pluripotent, able to give rise to all lineages of the future embryo when reintroduced into an embryo or differentiated *in* vitro (Evans and Kaufman, 1981; Martin, 1981; Smith et al., 1988; Williams et al., 1988; Beddington and Robertson, 1989). ESCs are derived from the mammalian blastocyst at the stage when the inner cell mass (ICM) contains a heterogeneous mix of progenitors of two lineages, the epiblast (Epi) that will give rise to the embryo proper and primitive endoderm (PrE) that will give rise to the extraembryonic visceral and parietal endoderm (Chazaud et al., 2006). Like the ICM, ESC cultures are heterogeneous and contain populations primed towards both Epi and PrE (Chambers et al., 2007; Singh et al., 2007; Hayashi et al., 2008; Toyooka et al., 2008; Kobayashi et al., 2009; Canham et al., 2010). However, in ESC cultures these progenitors are in a dynamic equilibrium (Canham et al., 2010; Morgani et al., 2013; Morgani and Brickman, 2014; Posfai et al., 2014).

The *in vitro* culture of ESCs can be supported by a number of factors, but typically require LIF (Smith et al., 1988; Williams et al., 1988; Ying et al., 2003; Ying et al., 2008). In defined culture conditions, containing small molecule inhibitors of GSK3 and MAPK (2i) (Ying et al., 2008), LIF is required for efficient clonal expansion. However, when LIF is removed from 2i, ESCs do not differentiate hence it is a good cell culture system to study the immediate early effects of LIF in the absence of differentiation-related gene expression changes. In ESCs, LIF binds to a heterodimeric receptor complex comprised of the LIF receptor (LIFR) and Glycoprotein 130 (GP130). Binding to the receptor complex results in activation of JAK tyrosine kinases that, in turn, phosphorylate the transcription factor STAT3. This results in STAT3 dimerization and translocation to the nucleus where it can activate target genes (Hirai et al., 2011). While there are other signalling pathways downstream of LIF (Burdon et al., 2002; Liu et al., 2007; Anneren, 2008), activation of STAT3 is necessary and sufficient to support ESC self-renewal (Niwa et al., 1998; Matsuda et al., 1999). A second cytokine that acts through GP130 to activate JAK/STAT, IL-6, has also been implicated in pre-implantation development (Do et

al., 2013) and can replace LIF as a means to sustain ESC self-renewal (Yoshida et al., 1994).

Although LIF supports ESC self-renewal, under standard conditions embryonic mutations of LIF pathway components do not show pre-implantation phenotypes (Li et al., 1995; Ware et al., 1995; Takeda et al., 1997; Nichols et al., 2001; Do et al., 2013). However, certain mammals have the ability to reversibly arrest development at the blastocyst stage as a result of suboptimal conditions e.g. nutrient scarcity, a phenomena known as diapause. Development can subsequently resume under more favourable conditions. Diapause can therefore be seen as a developmental mechanism to support sustained pluripotency and the induction of diapause can be used to improve ESC derivation (Nichols et al., 2001). When diapause is induced, *gp130*$^{-/-}$ embryos exhibit a complete loss of the pluripotent Epi population (Nichols et al., 2001) indicating that LIF may play a role *in vivo* in maintaining pluripotency, but that it is not required during normal embryonic development. However, it is also possible that JAK/STAT signalling is activated via a GP130-independent maternal mechanism during early development that masks a pre-implantation phenotype. Consistent with this, inhibiting downstream signalling, either through pharmacological inhibition of JAK or in embryos in which both maternal and zygotic *Stat3* have been removed, suggested that ICM maintenance requires active JAK/STAT signalling (Do et al., 2013).

Here we show that LIF acts through a two-pronged mechanism to support ICM expansion, both *in vivo* and *in vitro*, in ESCs. LIF acts to suppress Epi differentiation and also to support PrE expansion. We had previously demonstrated that LIF promotes the expansion of an extraembryonic-primed population of cells within ESC cultures (Morgani et al., 2013), consistent with its well-characterised role in extraembryonic development and implantation (Stewart et al., 1992; Takahashi et al., 2003; Poehlmann et al., 2005; Prakash et al., 2011). Here we show that LIF supports this population via JAK/STAT signalling, the same pathway that promotes ESC self-renewal (Niwa et al., 1998; Matsuda et al., 1999). We find that STAT3 phosphorylation correlates with a PrE rather than Epi identity *in vivo*, and that LIF stimulates PrE survival and proliferation, while inhibition of JAK activity leads to enhanced apoptosis in the PrE. We hypothesise that LIF maintains ESC self-renewal

and ICM expansion by enhancing the survival of an extraembryonic-primed population that provides paracrine factors for Epi expansion.

Results

LIF promotes an extraembryonic ESC population through the JAK/STAT pathway

We have previously shown that LIF promotes a population of ESCs primed towards an extraembryonic fate (Morgani et al., 2013), marked by the expression of a highly sensitive fluorescent reporter for the endoderm marker *Hhex* (*Hhex*-Venus (HV)) (Canham et al., 2010). We asked if this was a general property of signalling through GP130, as other members of the same cytokine family e.g. IL-6 have also been associated with self-renewal (Conover et al., 1993; Rose et al., 1994; Wolf et al., 1994; Yoshida et al., 1994; Pennica et al., 1995). Figure 1A shows that, not only can IL-6 induce HV expression, but also at a high dose it induces elevated levels of this transgene compared to LIF treatment. HV ESCs were cultured in 2i, to prevent differentiation in the absence of LIF, with increasing doses of IL-6. Expression of the HV reporter was assessed by flow cytometry (Fig. 1A). As previously reported (Morgani et al 2013), we observed HV induction in 2i/LIF and obtained similar levels of HV expression with a low dose of IL-6 (500 ng/ml, Fig. 1A). At 1000 units, the effect of LIF on the HV population becomes saturated (Morgani et al., 2013), but HV expression can be further increased with high doses of IL-6 (1000 ng/ml, Fig. 1A).

LIF was previously shown to alter the relative number of actively proliferating cells within the embryonic and extraembryonic-primed ESC populations (Morgani et al., 2013). Consistent with this, when LIF was added to ESCs cultured in 2i, HV expression gradually increased over several days (Fig. S1A). This observation was confirmed by qRT-PCR with PrE genes exhibiting a delayed response to LIF, including *HHex*, *Hnf4a*, *Dab2* and *Sox17*, contrasting with the rapid response (within 1 hour) of the immediate early target of LIF signalling, *Socs3*, or the sharp threshold responses of LIF transcriptional components, *Stat3* and *Klf4*, at 8-24 hours (Fig. 1B). Although *Gata4* demonstrated an early response to LIF, as with other PrE markers, the expression change was gradual (Fig. 1B). Previous microarray data showed that LIF also increased the expression of extracellular matrix (ECM) genes associated with PrE development (Morgani et al., 2013). Here we observed that these genes also increased in expression at 8-24 hours (Fig. 1B, Fig. S1B). Interestingly, we observed

that mesoderm and ectoderm markers, including *Lhx1*, *Cdx2*, *Wnt3*, *Otx2* and *Fgf5*, were rapidly downregulated between 1-8 hours following LIF addition, prior to changes in PrE gene expression (Fig. 1B, Fig. S1B).

As LIF acts on multiple downstream pathways (Burdon et al., 2002; Liu et al., 2007; Anneren, 2008), we asked which pathway was required for HV induction. We found that JAK/STAT signalling, also critical for ESC self-renewal, supported the expansion of the HV PrE-primed population. HV ESCs were cultured in 2i or 2i/LIF medium in the presence of small molecule inhibitors of the PI3K (LY) and JAK/STAT (JAKi) pathways. After 3 days of culture in these conditions, HV ESCs were analysed by flow cytometry. Induction of HV was blocked by inhibition of JAK/STAT, but not PI3K (Fig. 1C). While GP130 can also signal through activation of MAPK, all cells were cultured in 2i, containing a block to MEK, and hence MAPK signalling was not required for the induction of HV expression in response to LIF.

We found that LIFR was expressed heterogeneously within ESC cultures (Fig. 1D) and at higher levels in the HV positive (HV^+) compared to the HV negative (HV^-) population (Fig. 1E). This suggests that the pathway may be differentially activated in PrE and Epi progenitors. Antibody staining of ESCs for the LIF targets (Bourillot et al., 2009; Niwa et al., 2009; van Oosten et al., 2012) phosphorylated STAT3 (pSTAT3) and KLF4 suggested that, while there is some overlap with expression of the Epi marker NANOG, this could not account for the all of the $KLF4^+$ or $pSTAT3^+$ cells. KLF4 expression was heterogeneous and showed some degree of coexpression with both NANOG and HV (Fig. 1F). Due to a lack of appropriate antibody combinations, we could not co-stain for pSTAT3 and HV. However, although there was some coexpression of pSTAT3 and NANOG, there were also cells that expressed high levels of NANOG but low levels of pSTAT3 and, vice versa, a fraction of cells that only expressed pSTAT3 (Fig. 1G), likely corresponding to the HV population.

pSTAT3 is associated with extraembryonic lineages in the pre-implantation embryo

We assessed the localisation of pSTAT3, and its target KLF4, throughout pre-implantation development and also quantified their expression within individual cells

using CellProfiler (Carpenter et al., 2006; Kamentsky et al., 2011) (Fig. 2,3). We validated this method by quantifying immunostaining of 3 well-characterised lineage markers NANOG (Epi), GATA6 (PrE) and CDX2 (trophoblast) (Fig. S2). Although there are low-levels of NANOG expression at the 2-cell stage (Fig. S2, Fig 2, 3), approximately 10-fold lower than in the late blastocyst, no obvious nuclear staining was observed suggesting that this is likely to be non-specific signal. Both inbred C57BL/6 and outbred CD1 mouse lines were analysed but, as results were comparable between different genetic backgrounds, data were combined (see methods). The analysis in Figure S2B shows the progressive segregation of these three lineages and suggests some new correlations, e.g. at the 8-cell stage all $NANOG^+$ cells are expressing CDX2, but not the reverse.

Strikingly, although there was an early correlation between NANOG and pSTAT3, this was lost by the late blastocyst stage (Fig. 2) after the PrE and Epi had segregated, prior to Epi differentiation. This contrasts with the overlap of NANOG with pSTAT3 that we observed in ESCs (Fig. 1G). As in ESCs, there was a correlation between KLF4 and NANOG although KLF4 was also expressed at low levels within the PrE (Fig. 3).

pSTAT3 is first observed in some, but not all, 2-cell embryos, but was present in all cells of the 8-cell morula (Fig. 2A,B). pSTAT3 was also observed in all cells until the early blastocyst stage (embryonic day (E) 3.5), when it became heterogeneous within the ICM and in some trophoblast cells (Fig. 2A). At this stage, pSTAT3 showed a strong correlation with both GATA6 and NANOG expression (Fig. 2A,B). By the late blastocyst stage (E 4.5), pSTAT3 and GATA6 remained correlated, and there was now a significant negative correlation between NANOG and pSTAT3 (Fig. 2B, * $p = 0.04$). pSTAT3 was expressed almost exclusively in the extraembryonic PrE and trophoblast and only at low levels within the Epi (Fig. 2A,B).

KLF4 was also expressed from the 2-cell stage and continued to be expressed in all cells until the early blastocyst stage (E3.5) (Fig. 3A,B). KLF4, as in ESCs, was then heterogeneously expressed, overlapping with both the $NANOG^+$ and $GATA6^+$ populations (Fig. 3A,B). In the late blastocyst (E4.5), KLF4 was expressed both in the Epi and PrE, although at a lower level in the PrE (Fig. 3A,B). As it is expressed

highly in the Epi, KLF4 appeared correlated with NANOG expression at this late blastocyst stage. We also quantified the correlation between pSTAT3 and KLF4 expression and observed that, while at the early blastocyst stage there is a correlation between this markers, this decreases by the late blastocyst (Fig. S3A,B).

Embryo culture in the presence of LIF promotes PrE cell expansion

As we observed that the JAK/STAT pathway promoted an extraembryonic fate in ESCs, and that pSTAT3 was associated with the extraembryonic lineages *in vivo*, we asked whether LIF could regulate lineage choice *in vivo*. Embryos were cultured from E2.5, for 3 days, until the late blastocyst (equivalent of E4.5 *in vivo*), the time period that the decision between Epi and PrE fates is being made, in the presence or absence of LIF. As shown in Figure 4, LIF produces an apparent increase in the fraction of $GATA6^{+}$ PrE, but has little affect on NANOG.

While the observation shown in Figure 4 is robust, there is a range of phenotypes and we wished to provide quantitative data on the impact of LIF on PrE vs. Epi specification. Based on counting cells in control ICMs, i.e. those cultured in only KSOM, we observed a fraction of embryos that had a significantly higher than average proportion of either $GATA6^{+}$ or $NANOG^{+}$ cells within the ICM (Fig. S4A,B, P = 0.0025 and 0.0003 respectively). As we observed a variation in the number of $GATA6^{+}$ and $NANOG^{+}$ positive cells within ICMs, we assigned embryos as '$GATA6^{Hi}$' and '$NANOG^{Hi}$' if the average proportion of $GATA6^{+}$ or $NANOG^{+}$ ICM cells was outside of one standard deviation of control embryos (Fig. S4A,B, S5A). Conversely, 'normal' embryos were within one standard deviation of the proportion of $GATA6^{+}$ or $NANOG^{+}$ ICM cells in controls (Fig. S4A,B, S5A). There was no significant difference in the total number of cells in embryos from each of these categories, indicating that this variation was not due to disparity of developmental stage (Fig. S4C). When embryos were cultured in the presence of LIF from E2.5 until the late blastocyst, we observed a corresponding increase in the level of pSTAT3 and in both the PrE and Epi (Fig. S5B). However, pSTAT3 continued to be present at levels approximately 3-fold higher in the PrE than in the Epi (Fig. S5B). KLF4 also showed an increase in expression in both Epi and PrE and was now expressed at similar levels in both cell types (Fig. S5B). We also found that the fraction of

GATA6^{Hi} embryos more than doubled, from 15% to approximately 40% (Fig. 4A,B, Fig. S5C-E). Similar observations were made when scoring based on GATA4 staining (Fig. S5F,G). Additionally, at higher doses of LIF, we observed a fraction of embryos that had only GATA6^{+} cells in the ICM ('GATA6 only', Fig. 4B, Fig. S5E). Treatment with LIF had no effect on the absolute number of trophoblast cells (Fig. S5H). We observed a similar increase in the proportion of GATA6^{+} cells when embryos were cultured from E1.5 or E3.5 until E4.5 (data not shown). In addition, we analysed LIF-treated embryos at earlier stages to determine how this phenotype developed over time. Following 1 day of culture in LIF, when embryos had reached the late morula stage, we observed no difference in the total number of cells in embryos (Fig. S5I). However, after 2 days of culture in LIF, at the early blastocyst stage, we observed a significant increase in both the total number of cells in the embryo (Fig. S5J) and the absolute number of GATA6^{+} PrE cells per embryo, but not in the number of NANOG^{+} Epi cells (Fig. S5K). Thus the increase in cell number was a result of an increase in the number of GATA6^{+} PrE cells in response to LIF and this was also represented by an increase in the proportion of GATA6^{Hi} embryos (Fig. 4C). Treatment with LIF also appeared to reduce the number of cells that had yet to commit to either lineage, as the population of cells co-expressing GATA6 and NANOG at these stages is reduced (Fig. 4C).

As we did not observe a decrease in the number of NANOG^{+} ICM cells (Fig. S5C), it seemed unlikely that LIF was directly acting on cell fate to switch ICM cells from Epi to PrE. Additionally, we had previously observed in ESCs (Morgani and Brickman, 2014) that LIF supported expansion of the PrE-primed population by a selective increase in proliferation. We therefore asked whether LIF was regulating the balance of cell types in the embryo by altering proliferation or apoptosis in either of these lineages. Embryos were cultured from E2.5-E4.5 in the presence or absence of LIF and immunostained for NANOG, GATA6 and CDX2, as well as for a marker of dividing cells, phospho Ser10 HISTONE H3 (pHH3). In the presence of LIF, a slight but significant increase in proliferation was observed in GATA6^{Hi} embryos (Fig. 4D, $P = 0.0492$). To assess the level of apoptosis we immunostained E4.5 embryos for the 3 lineage markers as well as CLEAVED CASPASE-3 (CC3). In control, KSOM only conditions, we observed a significant increase in the number of apoptotic cells in GATA6^{Hi} embryos ($P = 0.0081$), which was decreased upon the addition of LIF (Fig.

4E,F). As the nuclear membrane is generally broken down in $CC3^+$ cells, transcription factor expression is lost and it was not possible to assign lineages to apoptotic cells. However, when scored on physical location, we observed a clear and significant decrease in apoptotic cells or debris positioned adjacent to or inside the cavity (potentially originating from PrE cells) which is also reflected in the relative increase in the proportion of apoptotic cells in the inside of the ICM (Fig. 4F-H, $P<0.0001$). There was no significant affect on proliferation or apoptosis in $NANOG^{Hi}$ embryos in the presence of LIF (Fig. 4D,E).

Blocking the JAK/STAT pathway leads to ICM defects including increased apoptosis in the PrE

As we had observed that the ability of LIF to promote a PrE-like population in ESC cultures was mediated by JAK/STAT signalling (Fig. 1C), we used a pharmacological inhibitor of JAK activity (JAKi) to assess the consequences of blocking this pathway for lineage segregation in the ICM. It was recently shown that culturing pre-implantation embryos in JAKi caused a generic defect in ICM maintenance (Do et al., 2013), and we wished to understand how this defect relates to PrE expansion. We therefore cultured embryos from E2.5-E4.5 in control conditions (KSOM) or in KSOM with JAKi. We titrated the inhibitor in ESCs and observed that, at doses previously reported (5 μM) (Do et al., 2013), we observed widespread cell death after 2 days (Fig. S6A,B). However, we found doses as low as 500 nM JAKi were sufficient to suppress STAT3 phosphorylation. In order to minimise toxicity to embryos, we cultured embryos at 500nM and 100 nM. At 500 nM JAKi, we observed no pSTAT3 in embryos and a reduction in KLF4 expression (Fig. S6C,D). At doses of 100 and 500 nM JAKi, we observed a decrease in the number of $NANOG^+$ cells and a slight decrease in the number of $GATA6^+$ ICM cells (Fig. 5A). However, we observed obvious phenotypes in approximately 50% of embryos including embryos cavitated without an ICM, embryos with a cavity where the Epi should be located but still maintaining a $GATA6^+$ PrE and embryos that had ICM cells that expressed neither NANOG, GATA6 nor CDX2 (Fig. 5B,C, Fig. S6E,F). Although these cells no longer expressed NANOG, they maintained expression of OCT4 (Fig. S6G), suggesting that they represent differentiated Epi. In addition, we saw an increase in the proportion of embryos that had only GATA6 or only NANOG within the ICM

(Fig. 5B, Fig. S6F). However, in embryos where there were only NANOG^{+} ICM cells, the number of ICM cells was also significantly decreased indicating Epi defects (Fig. S6F). Little effect was observed on the number of trophoblast cells (Fig. S6H) and, although there was a slight decrease in total cell number in embryos without an ICM or with cavities, this was not significant (Fig. S6I). To assess the point when these phenotypes first become apparent, we examined embryos that had been cultured in JAKi for one or two days. We observed no change in the total numbers of cells at the late morula or early blastocyst stages (Fig. S6J, K), but observed an equal increase in the number of GATA6^{Hi} and NANOG^{Hi} embryos in the early blastocyst (Fig S6L). As with the LIF-treated embryos, JAKi appeared to accelerate the resolution of Epi and PrE lineages, reducing the number of GATA6 and NANOG coexpressing cells at this earlier stage.

Apoptosis in GATA6^{Hi} embryos was still detected and slightly increased as a result of JAK inhibition (Fig. 5D,E). Additionally, we observed a significant increase in the fraction of apoptotic cells adjacent to or inside the cavity (presumably originated from PrE cells) (Fig. 5F, $P<0.05$).

Discussion

In this paper we have shown that STAT3 phosphorylation, while initially throughout the pre-implantation embryo, becomes localized to the PrE in the late blastocyst. This suggests a role of JAK/STAT in PrE specification that is consistent with our observations that LIF supports extraembryonic gene expression in ESCs. As the induction of extraembryonic gene expression *in vitro* was a delayed response, it suggests that JAK/STAT acts to support a PrE population rather than directly regulating PrE gene expression. Thus we observed that the activation of STAT3 could enhance the percentage of ESCs that experienced PrE priming and increase the proportion of PrE cells at blastocyst stages of development.

In addition to its action on PrE priming, we observed that LIF caused the rapid downregulation of mesoderm and ectoderm markers prior to the upregulation of PrE markers, consistent with the fact that the mesoderm marker *Lhx1* and numerous Wnt pathway components are direct targets of STAT3 (Kidder et al., 2008). This is in keeping with previous observations that ESCs can differentiate to PrE and form basement membrane in the presence of LIF, but that ectoderm differentiation is blocked (Murray and Edgar, 2001). It was previously suggested that MEK and GSK3 inhibitors in 2i/LIF lead to a downregulation of mesoderm and ectoderm, but not PrE, markers compared to standard serum culture conditions (Marks et al., 2012). However, our findings suggest that this effect may not be mediated by 2i alone but also by LIF. If LIF is able to suppress ectoderm and mesoderm differentiation, this may explain the ability of its primary target KLF4 to drive Epi stem cells back to a naïve mESC cell state (Guo et al., 2009). Thus, cells induced by JAKi *in vivo* that express neither GATA6 nor NANOG, but continue to express OCT4, may represent cells that have differentiated to later Epi derivatives. Taken together, our findings suggest that LIF acts in pre-implantation development to suppress block Epi differentiation and support a PrE progenitor population.

We had previously shown that LIF enhances the number of actively proliferating PrE cells *in vitro* (Morgani et al., 2013) and have shown here that it does this through the JAK/STAT pathway. *In vivo* LIF had a modest effect on proliferation, which might translate into a more robust PrE phenotype over time. However, our exploration of

LIF's role *in vivo* also suggests that it acts to suppress apoptosis in a class of embryos with an elevated proportion of GATA6 cells. Similarly, LIF has been shown to suppress context-dependent apoptosis in ESCs. ESCs have the capacity to eliminate cells based on genotype as they embark on differentiation, a process mediated by competitive apoptosis that is suppressed via LIF (Sancho et al., 2013). In ESCs the exit from self-renewal into differentiation triggers cell competition and associated apoptosis (de Beco et al., 2012; Levayer and Moreno, 2013; Wagstaff et al., 2013). Hence, perhaps selective apoptosis is triggered as a result of PrE differentiation and this is suppressed by limiting concentrations of LIF.

The trophoblast expresses *Lif* during embryonic development, and *Lifr* and *Gp130* are expressed within the ICM cells (Nichols et al., 1996). Recent single cell microarray data also shows that the *Lifr* is expressed at higher levels within PrE cells than Epi cells at E3.5 and E4.5 (Ohnishi et al., 2014), consistent with our data in HV ES cells. Moreover, this data reveals that *Il-6* is expressed in the Epi, although data on *Lif* expression is not clear (Ohnishi et al., 2014). In addition, it has been shown that LIF receptors are enriched within extraembryonic endoderm (XEN) stem cell cultures (Artus et al., 2012). This suggests that the number of LIF/IL-6 producing cells, outside of the PrE, calibrate the size of the PrE. When there is insufficient PrE, excess LIF prevents apoptosis and stimulates proliferation. However, if the PrE expands beyond a certain point, such that the available amount of LIF is not sufficient to support the size of the PrE, apoptosis ensues and the embryo recalibrates.

We also observed a requirement for JAK/STAT signalling in ICM formation. Similar observations have been made by Solter et al. (Do et al., 2013). Although we observed an effect of LIF on Epi differentiation in ESCs, we detected little change in pluripotent gene expression (Morgani et al., 2013). How then does JAK/STAT signalling support self-renewal of the ICM and ESCs? One of the principle GO terms to come out of our previous analysis of LIF stimulation (Morgani et al., 2013) was ECM components commonly produced by the PrE. Perhaps one mechanism by which LIF supports the expansion of the ICM is through the production of basement membrane required for its survival. It has been shown in ESCs that basement membrane is important to maintain ESCs in an undifferentiated state (Przybyla and Voldman, 2012). Additionally, the only way in which individual Epi cells can be

shown to generate ESC lines in the presence of a pharmacological block to PrE specification (inhibition of MEK) is by the provision of specific ECM components (Boroviak et al., 2014). We also rarely observed embryos (3/98) in which the number of $NANOG^+$ cells exceeded the number of $GATA6^+$ cells, suggesting that a critical mass of PrE is required to support Epi expansion. Thus, LIF could have two roles in supporting Epi expansion, a block to later differentiation as well as a paracrine support network that depends on the PrE.

As we found that LIF blocks later Epi differentiation, it is not surprising that the correlation between pSTAT3 and NANOG is lost at the late blastocyst stage, prior to Epi maturation. *In vivo*, JAK/STAT signalling may only be necessary to block Epi differentiation for a limited time window when the PrE is actively being specified in response to the production of FGF4 by $NANOG^+$ Epi cells (Messerschmidt and Kemler, 2010; Frankenberg et al., 2011). This differs from the activity of LIF in ESCs *in vitro*, where we observed pSTAT3 in both $NANOG^+$ Epi and HV^+ PrE-primed ESCs. However, ESCs exist in a state of perpetual expansion in which these early developmental differentiation decisions are blocked. As a result, the requirement for pSTAT3 in both populations is prolonged indefinitely.

Taken together our observations suggest that development of the three primary lineages is intricately and dynamically linked. The level of LIF secreted by the trophoblast and Epi (Nichols et al., 1996; Ohnishi et al., 2014) may specify the number of PrE cells within the ICM. High levels of PrE:Epi leads to apoptosis in the PrE whereas too little PrE would lead to a failure in Epi expansion as a result of reduced basement membrane. Our observation that accelerating PrE expansion through the manipulation of JAK/STAT signalling results in a loss of NANOG/GATA6 double positive cells in the ICM of early blastocysts, suggests that these sort of paracrine loops might have a selective role in the specification of both lineages from the point that differentiation begins in the first few cells. The combination of these two mechanisms would therefore be a means by which the embryo measures the relative levels of PrE and Epi and ensures that both lineages are present and correctly specified during Epi specification, expansion and during the initiation of patterning.

Materials and methods

ESC culture and flow cytometry

E14 and HV ESCs (129/Ola background) were used in this study. ESCs were maintained in serum/LIF or 2i medium (Morgani et al., 2013). *Stat3*$^{-/-}$ ESCs (a kind gift from J. Nichols) were maintained in 2i or 2iLIF. ESCs were also cultured in the presence of small molecule inhibitors, JAKi (5uM, Calbiochem), LY294002 (5uM, Promega), PD0325901 (1uM, Sigma).

Cells were collected by trypsinisation and stained for a marker of undifferentiated ESCs, Pecam-1 (1:400, BD Bioscience, APC conjugated, 551262) or SSEA-1 (DSHB, mc480) and DAPI (Invitrogen) to exclude dead cells (Canham et al., 2010; Morgani et al., 2013). The LIFR antibody (R&D, MAB5990) was used at 2.5 μg/10^6 cells and ESCs were stained for 30 minutes at room temperature before being washed and resuspended in FACs buffer with DAPI as described for other antibodies. Flow cytometry analysis was carried out using a BD LSR Fortessa. Analysis of data was done using FlowJo software (Tree Star) by gating on forward and side scatter to identify a cell population and eliminate debris, then gating DAPI negative, viable cells before assessing the level of Venus or APC.

ESC immunostaining

ESCs were cultured in 6-well plates on 25 mm glass coverslips coated with gelatin or in μ-slides (Ibidi). ESC immunostaining was carried out as previously described (Canham et al., 2010). For pStat3 staining, ESCs were permeabilised in methanol at -20°C for 5 minutes. Antibodies were used at the following concentrations Nanog (eBioscience, 14-5761) 1:200, anti-GFP Alexa488 conjugated (Molecular Probes, A21311) 1:200, Klf4 (R&D, AF3158) 1:200, pStat3 XP (Cell Signalling, 9145) 1:200. Coverslips were mounted onto glass slides using Vectashield mounting medium (Vector labs) and imaged by confocal microscopy using a Leica TCS SP8.

Mouse maintenance, embryo collection and culture

Both wild type inbred C57/BL6 and outbred CD1 mouse strains were used for these experiments. Animal work was carried in accordance with European legislation and was authorized by and carried out under Project License 2012-15-2934-00743 issued by the Danish Regulatory Authority. Mice were maintained in a 12-hour light/dark cycle in the designated facilities at the University of Copenhagen, Denmark. Natural matings were set up in the evening. Mice were checked for copulation plugs the following morning. Embryos were flushed in PB1 medium from oviducts between embryonic day (E) 1.5 and E2.5 and from the uterus at later stages. Where culturing was needed, embryos were cultured in KSOM medium (Millipore) to which different concentrations of LIF or JAKi inhibitor (Calbiochem) were added. The majority of embryos were flushed at E2.5. These embryos were then cultured for 3 days to reach the equivalent of an E4.5 *in vivo* embryo. The resulting embryos are labelled as E4.5. Embryos were cultured in distinct microdrops for each condition overlaid with embryo culture mineral oil (Sigma). Embryos were culture at 37°C, 5% CO2 and 90% humidity.

Embryo immunostaining and imaging

Immunostaining of embryos was carried out as previously described (Nichols et al., 2009). When using antibodies against phospho proteins, embryos were permeabilised in methanol at -20°C for 5 minutes. Primary antibodies were used at the following concentrations, Nanog (eBioscience) 1:200, Cdx2 (Biogenex, MU392A-UC) 1:200, Gata6 XP (Cell Signalling, 5851) 1:200, Gata6 (R&D, AF1700) 1:100, pStat3 XP (Cell Signalling) 1:200, Klf4 (R&D) 1:200, phospho-Histone H3 (Ser10) (Abcam, ab14955) 1:200, Cleaved Caspase-3 (Cell Signalling, 9664) 1:200, Gata4 (Santa Cruz, sc1237) 1:100. Embryos were imaged in an Attofluor chamber (Invitrogen) on a 25 mm coverslip using 20x magnification on a Leica TCS SP8 confocal.

Quantification of embryo immunostaining

Confocal immunostaining of embryos was quantified using open access software, CellProfiler (developed at MIT and the Broad Institute, USA, www.cellprofiler.org).

Individual cells stained by DAPI were identified using a manual selection tool. To determine pSTAT3 and KLF4 levels, after treatments, in PrE and Epi, GATA6 and NANOG staining respectively were used to identify nuclei. Entire E1.5 and E2.5 embryos were quantified whereas 2 distinct confocal z-planes were quantified per blastocyst stage embryo. The mean pixel intensity (measured in arbitrary units) was measured in each selected nuclei for all fluorescence channels allowing a measure of colocalisation of different markers. Results were plotted as scatter plots in GraphPad Prism software and correlation statistics and linear regression analysis were carried out to generate a line of best fit. Both C57BL/6 and CD1 embryos were utilised for quantification. As there was no obvious difference in the results between these strains, data were combined. Interestingly, we observed that NANOG expression turns on in only a subset of C57BL/6 blastomeres at the 8-cell stage whereas NANOG is present in all blastomeres of CD1 mice at the 8-cell stage.

Embryo categorisation

The number of $GATA6^{+}$ and $NANOG^{+}$ ICM cells was counted in each embryo. Control (KSOM cultured) and LIF-treated (KSOM + LIF cultured) embryos were categorised as 1. Normal, 2. $GATA6^{Hi}$, 3. GATA6 alone, 4. $NANOG^{Hi}$, 5. NANOG alone. Embryos were categorised as 'normal' if the ratio of $GATA6^{+}$:$NANOG^{+}$ cells was within the average +/- the standard deviation of control embryos. Embryos were scored as $GATA6^{Hi}$ if the proportion of $GATA6^{+}$ ICM cells was above this range and $NANOG^{Hi}$ is the proportion of $NANOG^{+}$ ICM cells was above this range. Embryos were scored as GATA6 or NANOG alone if the ICM consisted only of $GATA6^{+}$ or $NANOG^{+}$ cells. JAKi-treated embryos also exhibited distinct phenotypes hence were additionally categorised as 6. No ICM, 7. Cavity (if there is an empty space where the Epi should be, still surrounded by PrE cells), 8. ? cells (if there are unidentified cells within the ICM expressing neither GATA6, NANOG nor CDX2). Both C57BL/6 and CD1 embryos were utilised for quantification. As there was no obvious difference in the results between these strains, data were combined.

Statistical analysis

Statistical analysis was performed using the QuickCalc GraphPad website (http://www.graphpad.com/quickcalcs/index.cfm). For non-parametric data, two-tailed chi-square tests were performed. For parametric data, unpaired Student's t-tests were used to determine significance. *P* value (*P*) is shown wherever the difference between compared groups was significant. Due to low *n* values for some conditions, and as no apparent difference was observed, data from various LIF and JAKi concentrations was pooled for statistical analysis.

Author contributions

S.M.M. conceived of and executed experiments and wrote the paper with J.M.B.; J.M.B. designed and supervised experiments and wrote the paper with S.M.M.

Acknowledgements

We thank the entire Brickman lab, Kim Sneppen and Ala Trusina for critical discussion of this manuscript; Javier Martin Gonzalez, Kasper Bonderup and Gelo de la Cruz for technical assistance; Jennifer Nichols for reagents. This work was supported by grants from Human Frontier in Science Program (HSFP) and the Novo Nordisk Foundation Section for Basic Stem Cell Biology. S.M.M. was supported by a University of Copenhagen Studentship.

References

Anneren, C. (2008). Tyrosine kinase signalling in embryonic stem cells. *Clin Sci (Lond)* **115**, 43-55.

Artus, J., Douvaras, P., Piliszek, A., Isern, J., Baron, M. H. and Hadjantonakis, A. K. (2012). BMP4 signaling directs primitive endoderm-derived XEN cells to an extraembryonic visceral endoderm identity. *Developmental biology* **361**, 245-262.

Beddington, R. S. and Robertson, E. J. (1989). An assessment of the developmental potential of embryonic stem cells in the midgestation mouse embryo. *Development* **105**, 733-737.

Boroviak, T., Loos, R., Bertone, P., Smith, A. and Nichols, J. (2014). The ability of inner-cell-mass cells to self-renew as embryonic stem cells is acquired following epiblast specification. *Nature cell biology* **16**, 516-528.

Bourillot, P. Y., Aksoy, I., Schreiber, V., Wianny, F., Schulz, H., Hummel, O., Hubner, N. and Savatier, P. (2009). Novel STAT3 target genes exert distinct roles in the inhibition of mesoderm and endoderm differentiation in cooperation with Nanog. *Stem Cells* **27**, 1760-1771.

Burdon, T., Smith, A. and Savatier, P. (2002). Signalling, cell cycle and pluripotency in embryonic stem cells. *Trends in cell biology* **12**, 432-438.

Canham, M. A., Sharov, A. A., Ko, M. S. and Brickman, J. M. (2010). Functional heterogeneity of embryonic stem cells revealed through translational amplification of an early endodermal transcript. *PLoS biology* **8**, e1000379.

Carpenter, A. E., Jones, T. R., Lamprecht, M. R., Clarke, C., Kang, I. H., Friman, O., Guertin, D. A., Chang, J. H., Lindquist, R. A., Moffat, J. et al. (2006). CellProfiler: image analysis software for identifying and quantifying cell phenotypes. *Genome biology* **7**, R100.

Chambers, I., Silva, J., Colby, D., Nichols, J., Nijmeijer, B., Robertson, M., Vrana, J., Jones, K., Grotewold, L. and Smith, A. (2007). Nanog safeguards pluripotency and mediates germline development. *Nature* **450**, 1230-1234.

Chazaud, C., Yamanaka, Y., Pawson, T. and Rossant, J. (2006). Early lineage segregation between epiblast and primitive endoderm in mouse blastocysts through the Grb2-MAPK pathway. *Developmental cell* **10**, 615-624.

Conover, J. C., Ip, N. Y., Poueymirou, W. T., Bates, B., Goldfarb, M. P., DeChiara, T. M. and Yancopoulos, G. D. (1993). Ciliary neurotrophic factor maintains the pluripotentiality of embryonic stem cells. *Development* **119**, 559-565.

de Beco, S., Ziosi, M. and Johnston, L. A. (2012). New frontiers in cell competition. *Developmental dynamics : an official publication of the American Association of Anatomists* **241**, 831-841.

Do, D. V., Ueda, J., Messerschmidt, D. M., Lorthongpanich, C., Zhou, Y., Feng, B., Guo, G., Lin, P. J., Hossain, M. Z., Zhang, W. et al. (2013). A genetic and developmental pathway from STAT3 to the OCT4-NANOG circuit is essential for maintenance of ICM lineages in vivo. *Genes & development* **27**, 1378-1390.

Evans, M. J. and Kaufman, M. H. (1981). Establishment in culture of pluripotential cells from mouse embryos. *Nature* **292**, 154-156.

Frankenberg, S., Gerbe, F., Bessonnard, S., Belville, C., Pouchin, P., Bardot, O. and Chazaud, C. (2011). Primitive endoderm differentiates via a three-step mechanism involving Nanog and RTK signaling. *Developmental cell* **21**, 1005-1013.

Guo, G., Yang, J., Nichols, J., Hall, J. S., Eyres, I., Mansfield, W. and Smith, A. (2009). Klf4 reverts developmentally programmed restriction of ground state pluripotency. *Development* **136**, 1063-1069.
Hayashi, K., Lopes, S. M., Tang, F. and Surani, M. A. (2008). Dynamic equilibrium and heterogeneity of mouse pluripotent stem cells with distinct functional and epigenetic states. *Cell stem cell* **3**, 391-401.
Hirai, H., Karian, P. and Kikyo, N. (2011). Regulation of embryonic stem cell self-renewal and pluripotency by leukaemia inhibitory factor. *The Biochemical journal* **438**, 11-23.
Kamentsky, L., Jones, T. R., Fraser, A., Bray, M. A., Logan, D. J., Madden, K. L., Ljosa, V., Rueden, C., Eliceiri, K. W. and Carpenter, A. E. (2011). Improved structure, function and compatibility for CellProfiler: modular high-throughput image analysis software. *Bioinformatics* **27**, 1179-1180.
Kidder, B. L., Yang, J. and Palmer, S. (2008). Stat3 and c-Myc genome-wide promoter occupancy in embryonic stem cells. *PloS one* **3**, e3932.
Kobayashi, T., Mizuno, H., Imayoshi, I., Furusawa, C., Shirahige, K. and Kageyama, R. (2009). The cyclic gene Hes1 contributes to diverse differentiation responses of embryonic stem cells. *Genes & development* **23**, 1870-1875.
Levayer, R. and Moreno, E. (2013). Mechanisms of cell competition: themes and variations. *The Journal of cell biology* **200**, 689-698.
Li, M., Sendtner, M. and Smith, A. (1995). Essential function of LIF receptor in motor neurons. *Nature* **378**, 724-727.
Liu, N., Lu, M., Tian, X. and Han, Z. (2007). Molecular mechanisms involved in self-renewal and pluripotency of embryonic stem cells. *Journal of cellular physiology* **211**, 279-286.
Marks, H., Kalkan, T., Menafra, R., Denissov, S., Jones, K., Hofemeister, H., Nichols, J., Kranz, A., Stewart, A. F., Smith, A. et al. (2012). The transcriptional and epigenomic foundations of ground state pluripotency. *Cell* **149**, 590-604.
Martin, G. R. (1981). Isolation of a pluripotent cell line from early mouse embryos cultured in medium conditioned by teratocarcinoma stem cells. *Proceedings of the National Academy of Sciences of the United States of America* **78**, 7634-7638.
Matsuda, T., Nakamura, T., Nakao, K., Arai, T., Katsuki, M., Heike, T. and Yokota, T. (1999). STAT3 activation is sufficient to maintain an undifferentiated state of mouse embryonic stem cells. *The EMBO journal* **18**, 4261-4269.
Messerschmidt, D. M. and Kemler, R. (2010). Nanog is required for primitive endoderm formation through a non-cell autonomous mechanism. *Developmental biology* **344**, 129-137.
Morgani, S. M. and Brickman, J. M. (2014). The molecular underpinnings of totipotency. *Philosophical transactions of the Royal Society of London. Series B, Biological sciences* **369**.
Morgani, S. M., Canham, M. A., Nichols, J., Sharov, A. A., Migueles, R. P., Ko, M. S. and Brickman, J. M. (2013). Totipotent embryonic stem cells arise in ground-state culture conditions. *Cell reports* **3**, 1945-1957.
Murray, P. and Edgar, D. (2001). The regulation of embryonic stem cell differentiation by leukaemia inhibitory factor (LIF). *Differentiation; research in biological diversity* **68**, 227-234.
Nichols, J., Chambers, I., Taga, T. and Smith, A. (2001). Physiological rationale for responsiveness of mouse embryonic stem cells to gp130 cytokines. *Development* **128**, 2333-2339.

Nichols, J., Silva, J., Roode, M. and Smith, A. (2009). Suppression of Erk signalling promotes ground state pluripotency in the mouse embryo. *Development* **136**, 3215-3222.
Nichols, J., Davidson, D., Taga, T., Yoshida, K., Chambers, I. and Smith, A. (1996). Complementary tissue-specific expression of LIF and LIF-receptor mRNAs in early mouse embryogenesis. *Mechanisms of development* **57**, 123-131.
Niwa, H., Burdon, T., Chambers, I. and Smith, A. (1998). Self-renewal of pluripotent embryonic stem cells is mediated via activation of STAT3. *Genes & development* **12**, 2048-2060.
Niwa, H., Ogawa, K., Shimosato, D. and Adachi, K. (2009). A parallel circuit of LIF signalling pathways maintains pluripotency of mouse ES cells. *Nature* **460**, 118-122.
Ohnishi, Y., Huber, W., Tsumura, A., Kang, M., Xenopoulos, P., Kurimoto, K., Oles, A. K., Arauzo-Bravo, M. J., Saitou, M., Hadjantonakis, A. K. et al. (2014). Cell-to-cell expression variability followed by signal reinforcement progressively segregates early mouse lineages. *Nature cell biology* **16**, 27-37.
Pennica, D., Shaw, K. J., Swanson, T. A., Moore, M. W., Shelton, D. L., Zioncheck, K. A., Rosenthal, A., Taga, T., Paoni, N. F. and Wood, W. I. (1995). Cardiotrophin-1. Biological activities and binding to the leukemia inhibitory factor receptor/gp130 signaling complex. *The Journal of biological chemistry* **270**, 10915-10922.
Poehlmann, T. G., Fitzgerald, J. S., Meissner, A., Wengenmayer, T., Schleussner, E., Friedrich, K. and Markert, U. R. (2005). Trophoblast invasion: tuning through LIF, signalling via Stat3. *Placenta* **26 Suppl A**, S37-41.
Posfai, E., Tam, O. H. and Rossant, J. (2014). Mechanisms of pluripotency in vivo and in vitro. *Current topics in developmental biology* **107**, 1-37.
Prakash, G. J., Suman, P., Morales Prieto, D. M., Markert, U. R. and Gupta, S. K. (2011). Leukaemia inhibitory factor mediated proliferation of HTR-8/SVneo trophoblast cells is dependent on activation of extracellular signal-regulated kinase 1/2. *Reproduction, fertility, and development* **23**, 714-724.
Przybyla, L. M. and Voldman, J. (2012). Attenuation of extrinsic signaling reveals the importance of matrix remodeling on maintenance of embryonic stem cell self-renewal. *Proceedings of the National Academy of Sciences of the United States of America* **109**, 835-840.
Rose, T. M., Weiford, D. M., Gunderson, N. L. and Bruce, A. G. (1994). Oncostatin M (OSM) inhibits the differentiation of pluripotent embryonic stem cells in vitro. *Cytokine* **6**, 48-54.
Sancho, M., Di-Gregorio, A., George, N., Pozzi, S., Sanchez, J. M., Pernaute, B. and Rodriguez, T. A. (2013). Competitive interactions eliminate unfit embryonic stem cells at the onset of differentiation. *Developmental cell* **26**, 19-30.
Singh, A. M., Hamazaki, T., Hankowski, K. E. and Terada, N. (2007). A heterogeneous expression pattern for Nanog in embryonic stem cells. *Stem Cells* **25**, 2534-2542.
Smith, A. G., Heath, J. K., Donaldson, D. D., Wong, G. G., Moreau, J., Stahl, M. and Rogers, D. (1988). Inhibition of pluripotential embryonic stem cell differentiation by purified polypeptides. *Nature* **336**, 688-690.
Stewart, C. L., Kaspar, P., Brunet, L. J., Bhatt, H., Gadi, I., Kontgen, F. and Abbondanzo, S. J. (1992). Blastocyst implantation depends on maternal expression of leukaemia inhibitory factor. *Nature* **359**, 76-79.

Takahashi, Y., Carpino, N., Cross, J. C., Torres, M., Parganas, E. and Ihle, J. N. (2003). SOCS3: an essential regulator of LIF receptor signaling in trophoblast giant cell differentiation. *The EMBO journal* **22**, 372-384.
Takeda, K., Noguchi, K., Shi, W., Tanaka, T., Matsumoto, M., Yoshida, N., Kishimoto, T. and Akira, S. (1997). Targeted disruption of the mouse Stat3 gene leads to early embryonic lethality. *Proceedings of the National Academy of Sciences of the United States of America* **94**, 3801-3804.
Toyooka, Y., Shimosato, D., Murakami, K., Takahashi, K. and Niwa, H. (2008). Identification and characterization of subpopulations in undifferentiated ES cell culture. *Development* **135**, 909-918.
van Oosten, A. L., Costa, Y., Smith, A. and Silva, J. C. (2012). JAK/STAT3 signalling is sufficient and dominant over antagonistic cues for the establishment of naive pluripotency. *Nature communications* **3**, 817.
Wagstaff, L., Kolahgar, G. and Piddini, E. (2013). Competitive cell interactions in cancer: a cellular tug of war. *Trends in cell biology* **23**, 160-167.
Ware, C. B., Horowitz, M. C., Renshaw, B. R., Hunt, J. S., Liggitt, D., Koblar, S. A., Gliniak, B. C., McKenna, H. J., Papayannopoulou, T., Thoma, B. et al. (1995). Targeted disruption of the low-affinity leukemia inhibitory factor receptor gene causes placental, skeletal, neural and metabolic defects and results in perinatal death. *Development* **121**, 1283-1299.
Williams, R. L., Hilton, D. J., Pease, S., Willson, T. A., Stewart, C. L., Gearing, D. P., Wagner, E. F., Metcalf, D., Nicola, N. A. and Gough, N. M. (1988). Myeloid leukaemia inhibitory factor maintains the developmental potential of embryonic stem cells. *Nature* **336**, 684-687.
Wolf, E., Kramer, R., Polejaeva, I., Thoenen, H. and Brem, G. (1994). Efficient generation of chimaeric mice using embryonic stem cells after long-term culture in the presence of ciliary neurotrophic factor. *Transgenic research* **3**, 152-158.
Ying, Q. L., Nichols, J., Chambers, I. and Smith, A. (2003). BMP induction of Id proteins suppresses differentiation and sustains embryonic stem cell self-renewal in collaboration with STAT3. *Cell* **115**, 281-292.
Ying, Q. L., Wray, J., Nichols, J., Batlle-Morera, L., Doble, B., Woodgett, J., Cohen, P. and Smith, A. (2008). The ground state of embryonic stem cell self-renewal. *Nature* **453**, 519-523.
Yoshida, K., Chambers, I., Nichols, J., Smith, A., Saito, M., Yasukawa, K., Shoyab, M., Taga, T. and Kishimoto, T. (1994). Maintenance of the pluripotential phenotype of embryonic stem cells through direct activation of gp130 signalling pathways. *Mechanisms of development* **45**, 163-171.

Figures

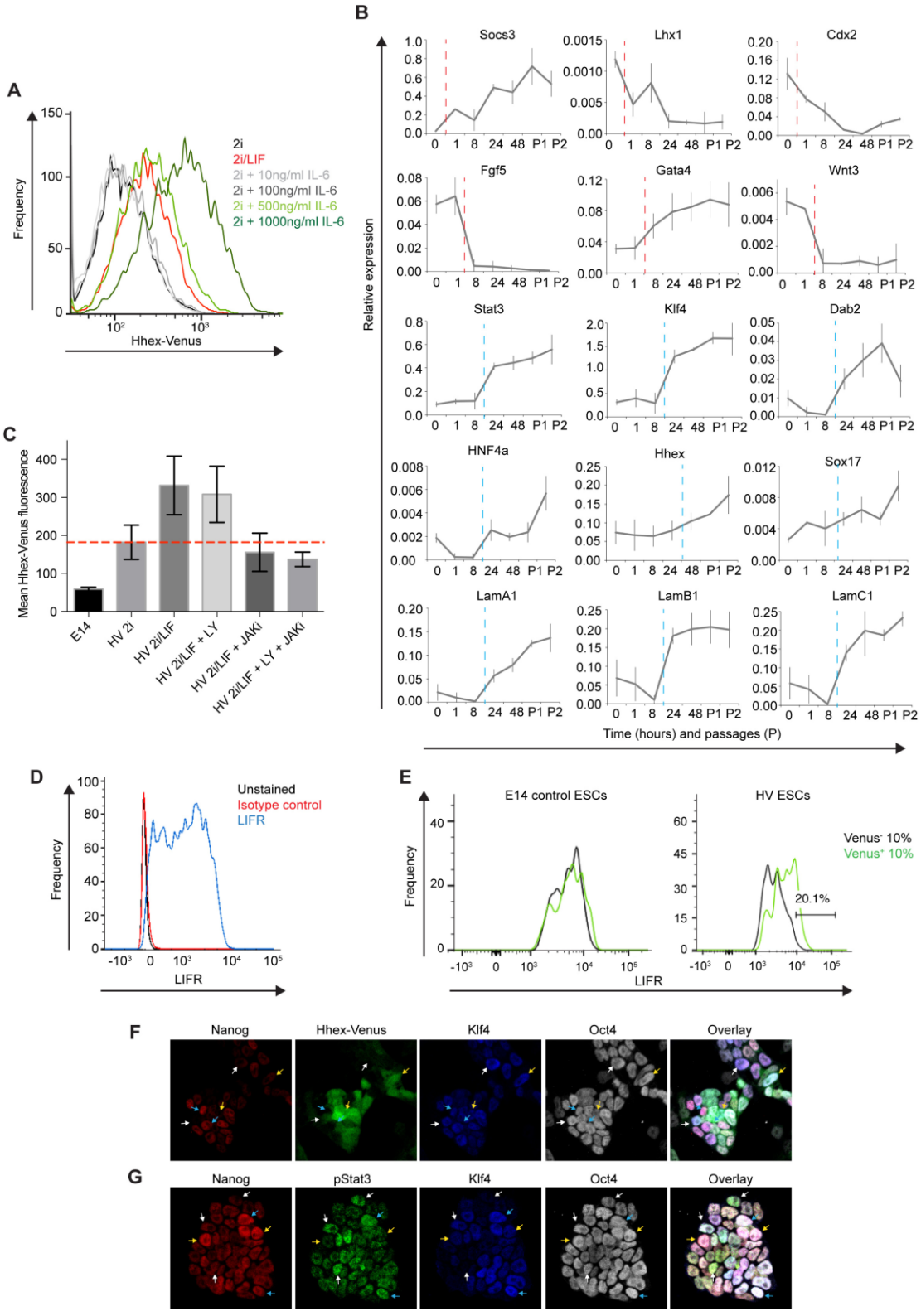

Figure 1. LIF and IL-6 promote the expansion of an extraembryonic-primed ESC population through the JAK/STAT pathway. A. Flow cytometry histogram of HV ESCs cultured in 2i, 2i/LIF or 2i with increasing doses of IL-6. **B.** qRT-PCR time

course of ESCs cultured in 2i for 3 passages before adding LIF for up to 2 passages. Data is shown relative to the geometric mean of the housekeeping genes, TBP and PGK1. Values represent the mean +/- the s.d. of 3 biological replicates of independent ESC lines. Red dotted lines indicate genes that are early responders to LIF (1-8 hours) while blue dotted lines indicate later responders (8 hours onwards). **C.** Mean HV fluorescence, detected by flow cytometry, after HV ESCs were cultured for 3 days in 2i/LIF in the presence of small molecule inhibitors of the PI3K (LY) and JAK/STAT (JAKi) pathways. Dotted line indicates the basal level of HV fluorescence in 2i cultures. **D-E.** Histogram showing flow cytometry analysis of HV ESCs antibody stained for the LIFR. Only cells expressing the marker of undifferentiated ESCs, SSEA-1, were analysed for the expression of the LIFR. Either the total population was analysed (**D**) or else the top (HV^+) and bottom (HV^-) 10% of HV-expressing cells were selected and analysed (**E**) for the expression of LIFR. The top and bottom 10% of HV expression was also selected in unstained and isotype control samples (see Fig S1C) as well as Venus fluorescence in the E14 cell line without the HV reporter, where any difference in signal would correspond to autofluorescence. **F.** Confocal optical sections of HV ESCs, cultured in serum/LIF, immunostained for NANOG, HV and KLF4. White arrows indicate cells expressing low levels of NANOG but high levels of KLF4. Yellow arrows indicate cells expressing high levels of KLF4 and HV but low levels of NANOG. Blue arrows indicate cells that express high levels of both NANOG and KLF4. **G.** Confocal optical sections of E14 ESCs, cultured in serum/LIF, immunostained for NANOG, pSTAT3 and KLF4. White arrows indicate cells expressing low levels of NANOG but high levels of pSTAT3. Yellow arrows indicate cells expressing high levels of NANOG but low levels of pSTAT3. Blue arrows indicate cells that express high levels of NANOG and pSTAT3.

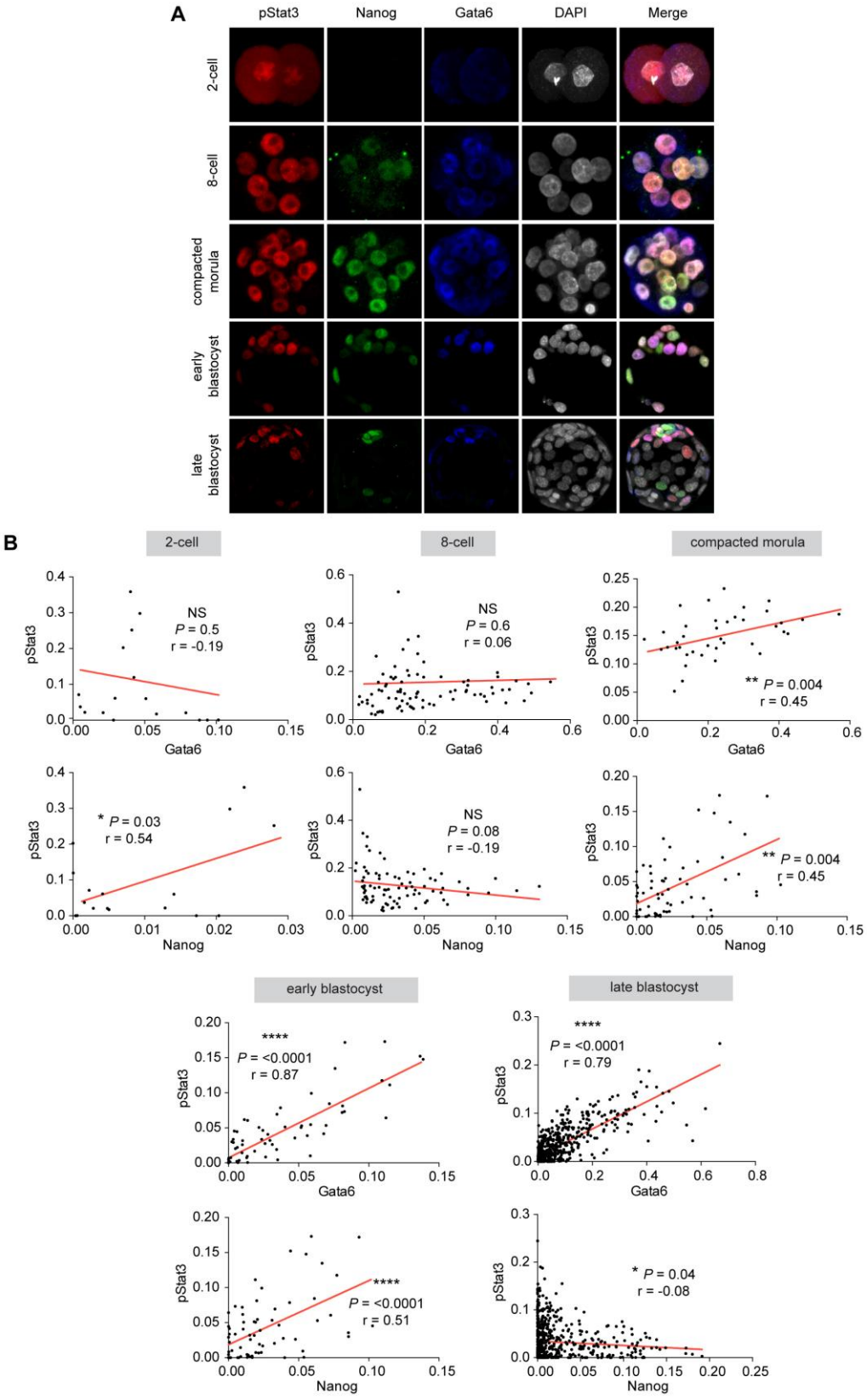

Figure 2. pSTAT3 is associated with extraembryonic lineages in the pre-implantation embryo. A. Immunostaining of embryos at different stages of pre-implantation development. Images from blastocyst-stage embryos represent confocal

optical sections through the ICM while images of earlier stages are extended focus showing the entire embryo. **B.** Quantification of colocalisation of NANOG, GATA6 and pSTAT3 during pre-implantation development. CellProfiler was used to quantify immunostaining in individual cells. Cell nuclei were identified by manual selection and the mean pixel intensity measured in arbitrary units of intensity (a.u.). Each point represents the intensity of the noted markers within a single nucleus. Linear regression line is shown in red. *P* values indicate correlation.

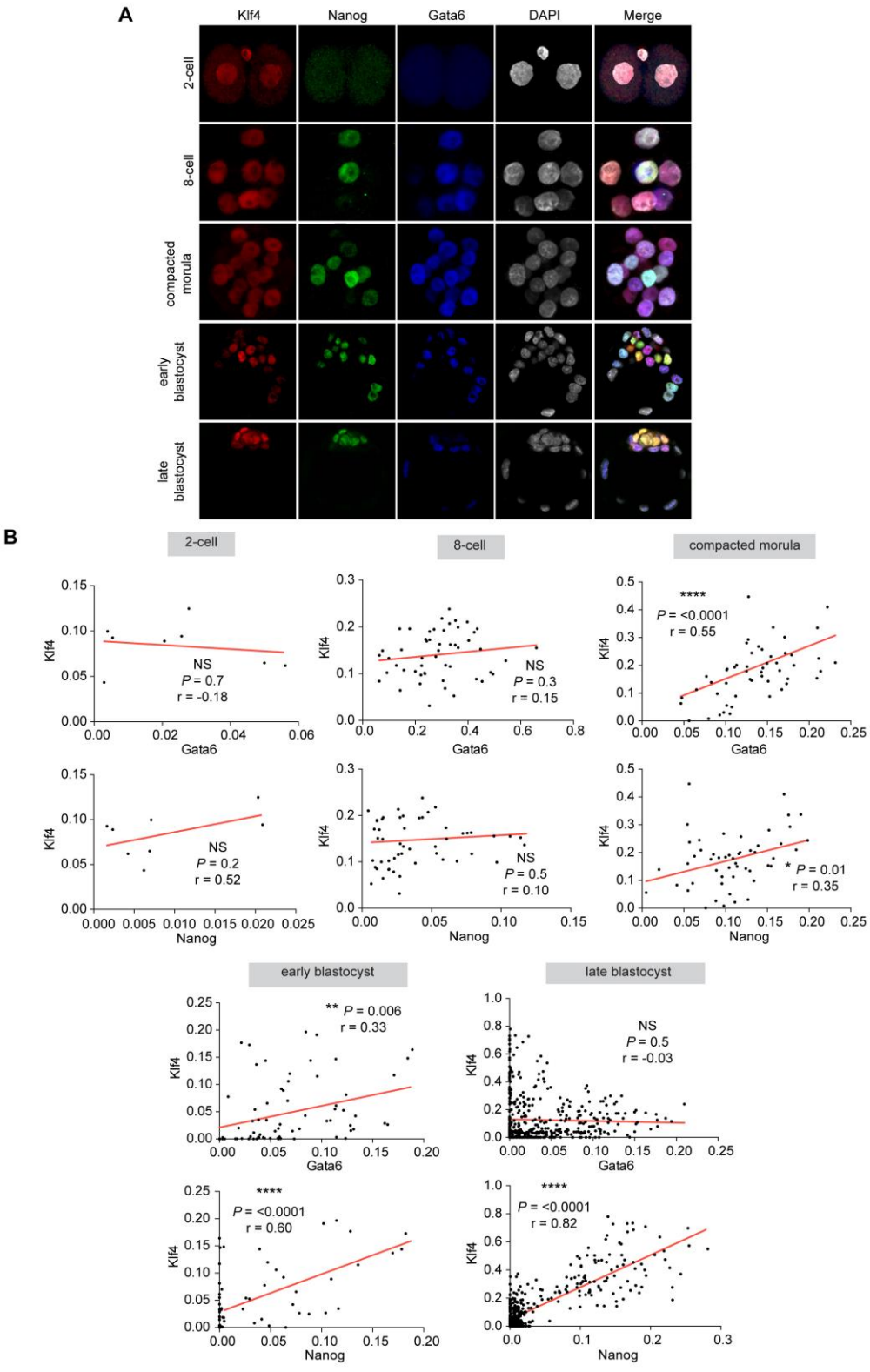

Figure 3. KLF4 is expressed in both the Epi and PrE. A. Immunostaining of embryos at different stages of pre-implantation development. Images from blastocyst-stage embryos represent confocal optical sections through the ICM while images of earlier stages are extended focus showing the entire embryo. **B.** Quantification of

colocalisation of NANOG, GATA6 and KLF4 during pre-implantation development. CellProfiler was used to quantify immunostaining in individual cells. Cell nuclei were identified by manual selection and the mean pixel intensity measured in arbitrary units of intensity (a.u.). Each point represents the intensity of the noted markers within a single nucleus. Linear regression line is shown in red. *P* values indicate correlation.

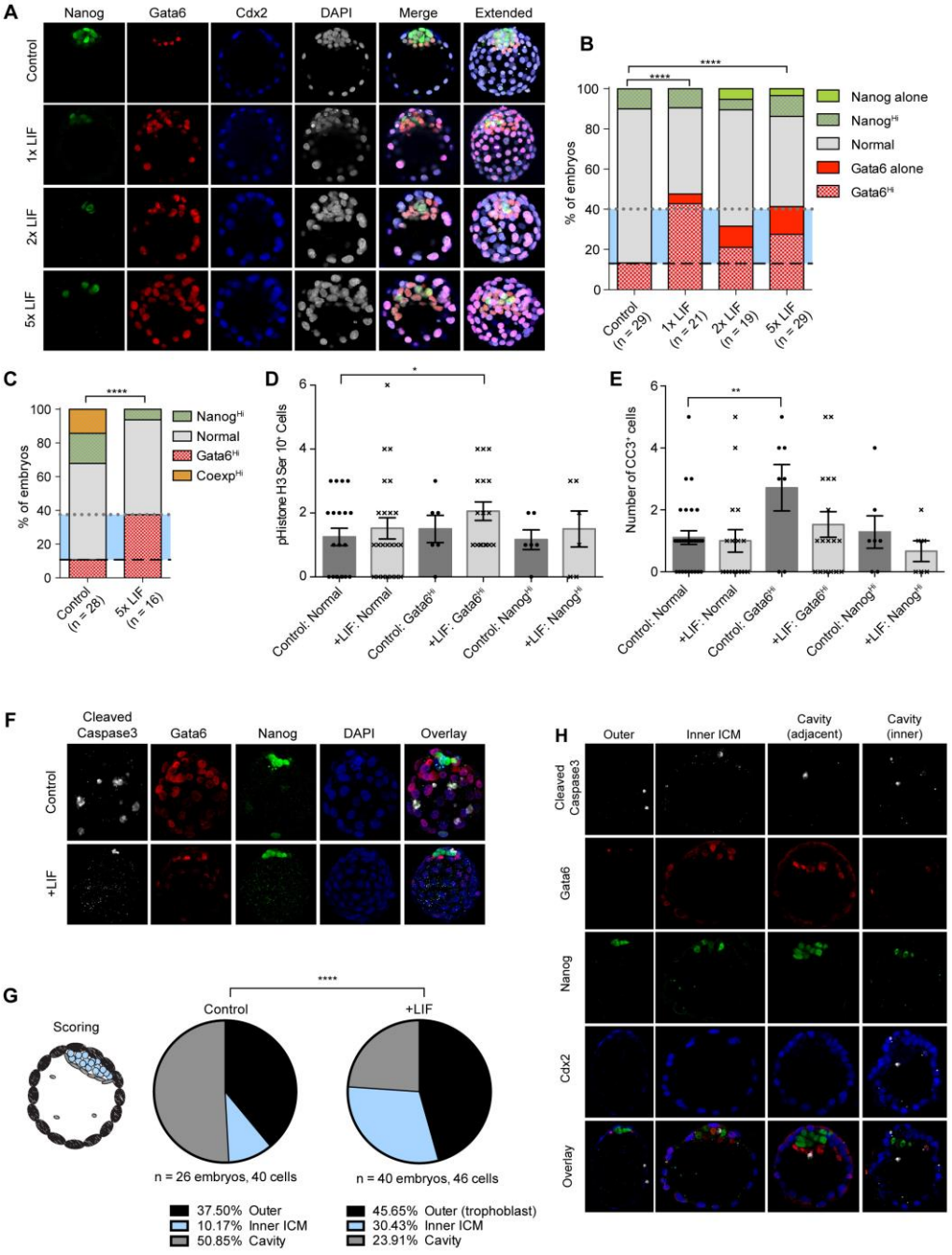

Figure 4. Embryos cultured with LIF show an increased proportion of PrE cells. Embryos were flushed from oviducts at E2.5 and cultured for 3 days in KSOM with increasing doses of LIF, 1000 U (1x), 2000 U (2x), 5000 U (5x). **A.** Confocal optical sections through the ICM of late blastocysts immunostained for the 3 lineage markers, NANOG (Epi), GATA6 (PrE) and CDX2 (trophoblast). An extended focus image also shows the whole embryo. **B-C.** Graphs showing categorisation of immunostained embryos. Embryos were cultured in KSOM or KSOM + LIF for 3 days **(B)** or 2 days

(C). The ICM of embryos was analysed based on the proportion of $GATA6^{+}$ and $NANOG^{+}$ cells. Normal embryos are those with the same proportions of PrE and Epi cells as the proportions +/- the s.d. in control (KSOM-cultured) embryos. $GATA6^{Hi}$ or $NANOG^{Hi}$ categories correspond to embryos that fell outside of the average control proportions +/- the s.d. due to having more $GATA6^{+}$ or $NANOG^{+}$ cells. For embryos after 2 days of culture, cells that coexpressed NANOG and GATA6 were quantified in the same manner. The number of embryos analysed is shown below each bar. The dashed black line indicates the proportion of $GATA6^{Hi}$ embryos in control conditions. The dotted line indicates the average number of embryos with high levels of GATA6 ($GATA6^{Hi}$, combined with GATA6 alone) embryos across all LIF treatments. . ****P<0.0001, two-tailed chi-square test. **D.** Graph displaying the average number of PHOSPHO-HISTONE H3 $(Ser10)^{+}$ cells (dividing cells) within E4.5 blastocysts. Error bars represent average +/- s.e.m. *P = 0.0492, Student's unpaired t-test. **E.** Graph displaying the average number of CLEAVED CASPASE-3 $(CC3)^{+}$ cells (apoptotic cells) within E4.5 blastocysts after culture from E2.5 +/- LIF. Error bars represent average +/- s.e.m. **P = 0.0081, Student's unpaired t-test. **F.** Confocal image projections of whole embryos immunostained for NANOG, GATA6 and CC3. **G.** Confocal optical sections of embryos immunostained for NANOG, GATA6, CDX2 and CC3 demonstrating scoring categories for location of apoptotic cells, either outer trophoblast cells, inner ICM or in the cavity either adjacent to the ICM or in the inner cavity. **H.** Graphs displaying the physical distribution of apoptotic cells within E4.5 blastocysts after culture from E2.5 +/- LIF, including a schematic diagram demonstrating the scoring criteria. 'Inner' cells are those observed within the inside of the ICM, 'outer' cells were those within the trophoblast and 'cavity' cells are those that were observed within the ICM adjacent to the cavity or within the cavity itself. ****P<0.0001, two-tailed chi-square test. As there was little difference between 1-5x LIF treatment, data were combined for panels D-G.

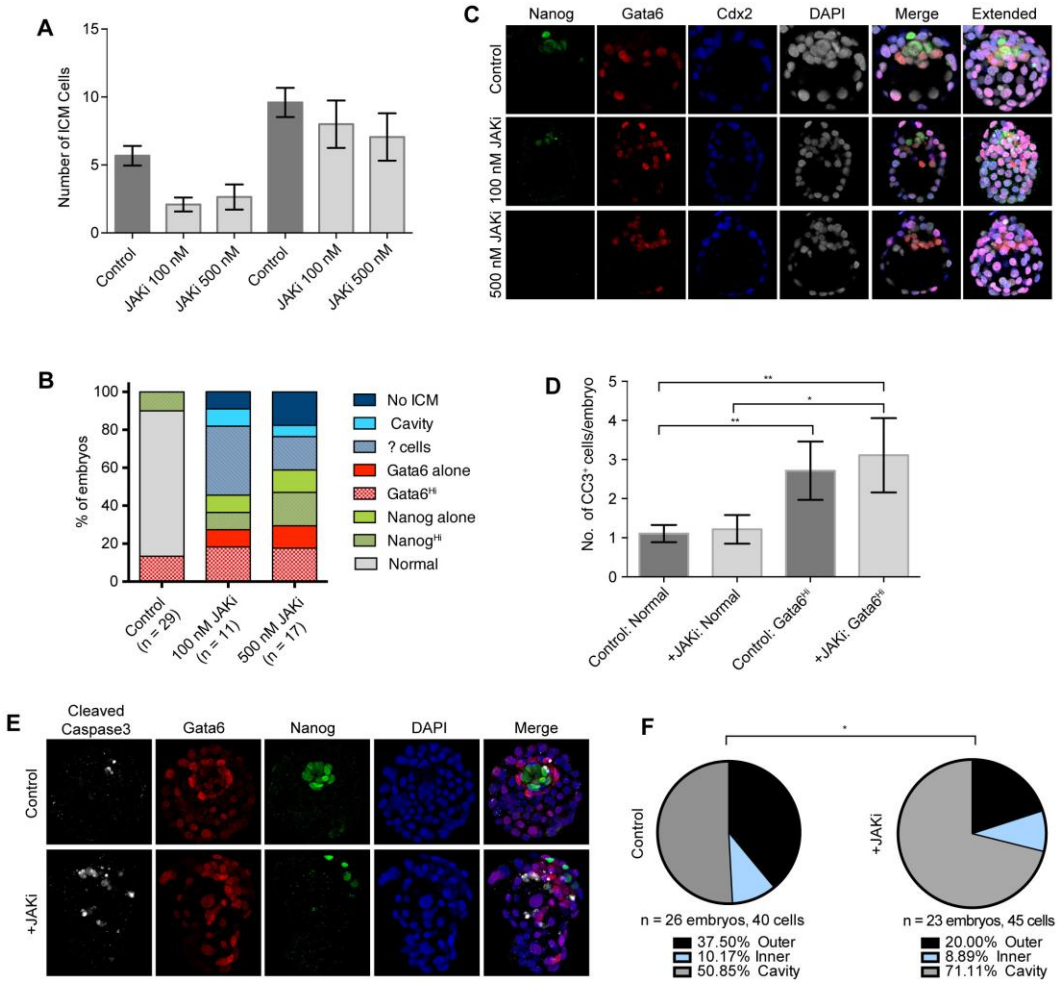

Figure 5. Embryos cultured with JAK inhibitor show varying phenotypes. Embryos were flushed from oviducts at E2.5 and cultured for 3 days in KSOM with 100 nM and 500 nM JAKi. **A.** Graph displaying the average number of NANOG^{+} and GATA6^{+} cells within the ICM of E4.5 blastocysts. Points represent individual embryos. Error bars represent average +/- s.e.m. **B.** Graph showing categorisation of immunostained embryos. The ICM of embryos was analysed based on the proportion of GATA6^{+} and NANOG^{+} cells. Normal embryos are those with the same proportions of PrE and Epi cells as the proportions +/- the s.d. in control (KSOM-cultured) embryos. GATA6^{Hi} or NANOG^{Hi} categories correspond to embryos that fell outside of the average control proportions +/- the s.d. due to having more GATA6^{+} or NANOG^{+} cells. '? cells' refers to embryos where cells were present within the ICM that expressed neither NANOG, GATA6 nor CDX2. The number below each bar indicates the number of embryos analysed. **C.** Confocal optical sections through the ICM of late blastocysts immunostained for the 3 lineage markers, NANOG (Epi),

GATA6 (PrE) and CDX2 (trophoblast). An extended focus image also shows the whole embryo. **D.** Graph displaying the average number of CLEAVED CASPASE-3 $(CC3)^{+}$ cells (apoptotic cells) within E4.5 blastocysts after culture from E2.5 +/- LIF. Error bars represent average +/- s.e.m. *P<0.05, ** P<0.01, Student's unpaired t-test. **E.** Confocal image projections of whole embryos immunostained for NANOG, GATA6 and CC3. **F.** Graphs displaying the physical distribution of apoptotic cells within E4.5 blastocysts after culture from E2.5 +/- 500 nM JAKi. 'Inner' cells are those observed within the inside of the ICM, 'outer' cells were those within the trophoblast and 'cavity' cells are those that were observed within the ICM adjacent to the cavity or within the cavity itself. *P<0.05, two-tailed chi-square test.

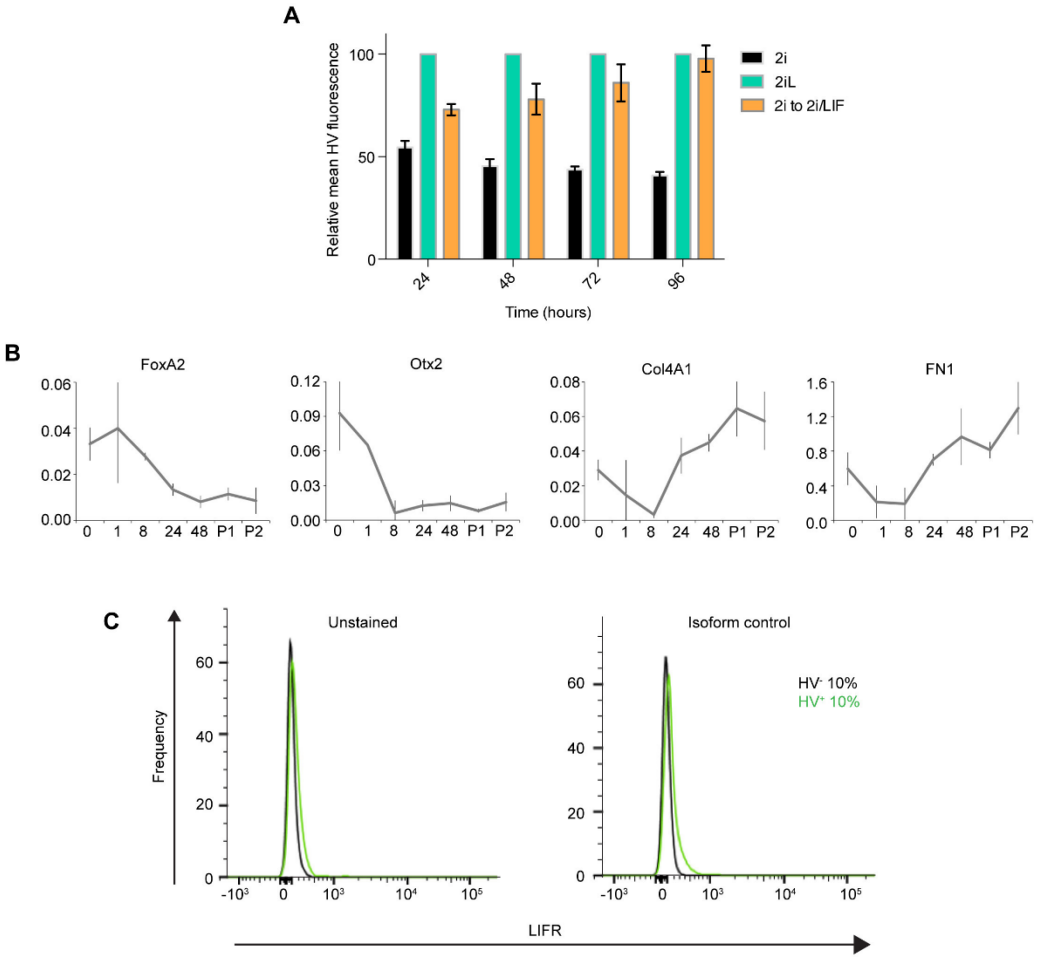

Supplementary Figure 1. A. HV ESCs were cultured in 2i or 2i/LIF for 3 passages. ESCs from 2i were then switched to 2i/LIF and the change in HV fluorescence was measured by flow cytometry each day. Data is shown relative to 2i/LIF mean fluorescence. Error bars represent the s.d. of 3 biological replicates. **B.** qRT-PCR time course of ESCs cultured in 2i for 3 passages before adding LIF for up to 3 passages. Data is shown relative to the geometric mean of the housekeeping genes, TBP and PGK1. Values represent the mean +/- the s.d. of 3 biological replicates of independent ESC lines. **C.** Histograms showing flow cytometry analysis of unstained ESCs or ESCs stained with an isotype control for the LIFR antibody as a control for LIFR flow cytometry in Fig. 1D,E. Only cells expressing the marker of undifferentiated ESCs, SSEA-1, were analysed for the expression of the LIFR. The top (HV^+) and bottom (HV^-) 10% of HV-expressing cells were selected and analysed for the expression of LIFR. Any difference in signal would correspond to autofluorescence.

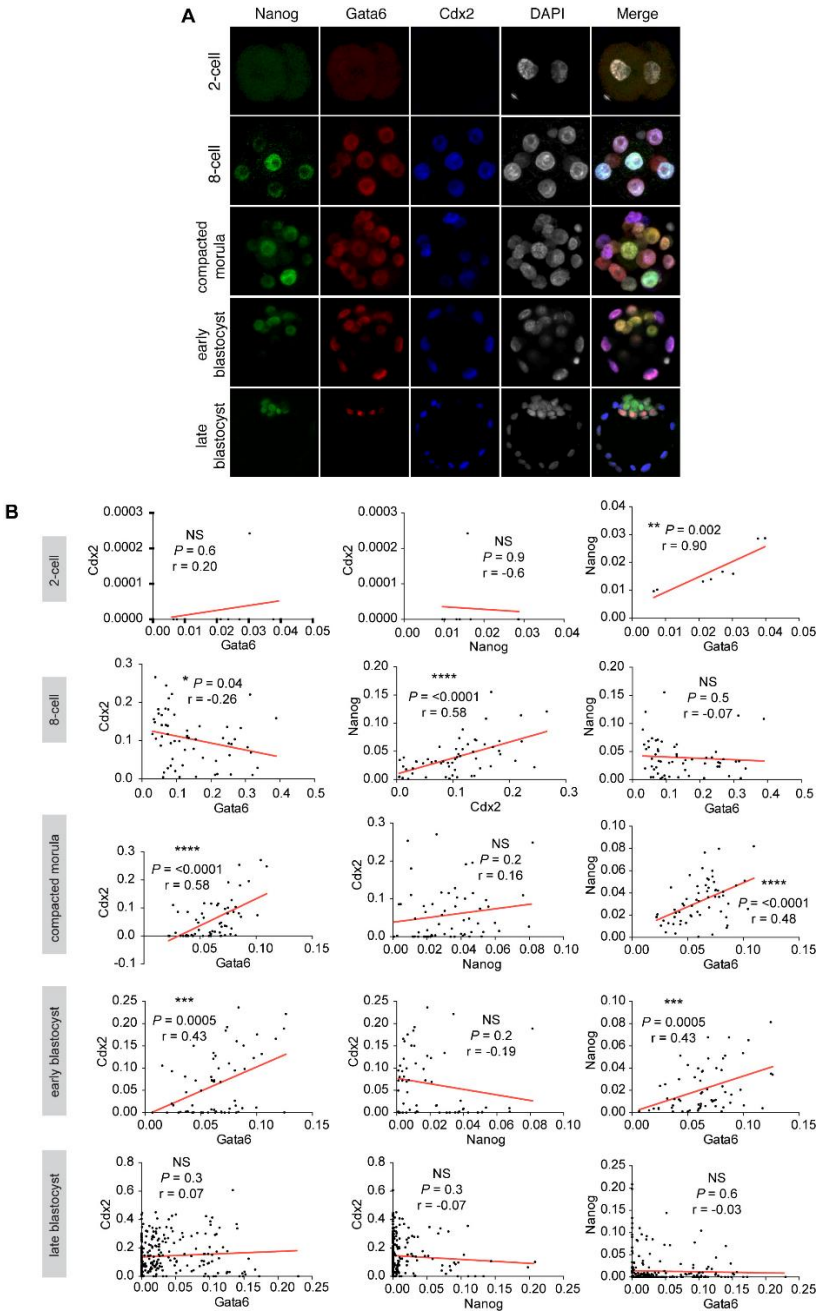

Supplementary Figure 2. Validation of coexpression quantification methodology. **A.** Immunostaining of embryos at different stages of pre-implantation development. Images from blastocyst-stage embryos represent confocal optical sections through the ICM while images of earlier stages are extended focus showing the entire embryo. **B.** Quantification of colocalisation of NANOG, GATA6 and CDX2 during pre-implantation development. CellProfiler was used to quantify immunostaining in individual cells. Cell nuclei were identified by manual selection and the mean pixel intensity measured in arbitrary units of intensity (a.u.). Each point represents the intensity of the noted markers within a single nucleus. Linear regression line is shown in red. *P* values indicate correlation.

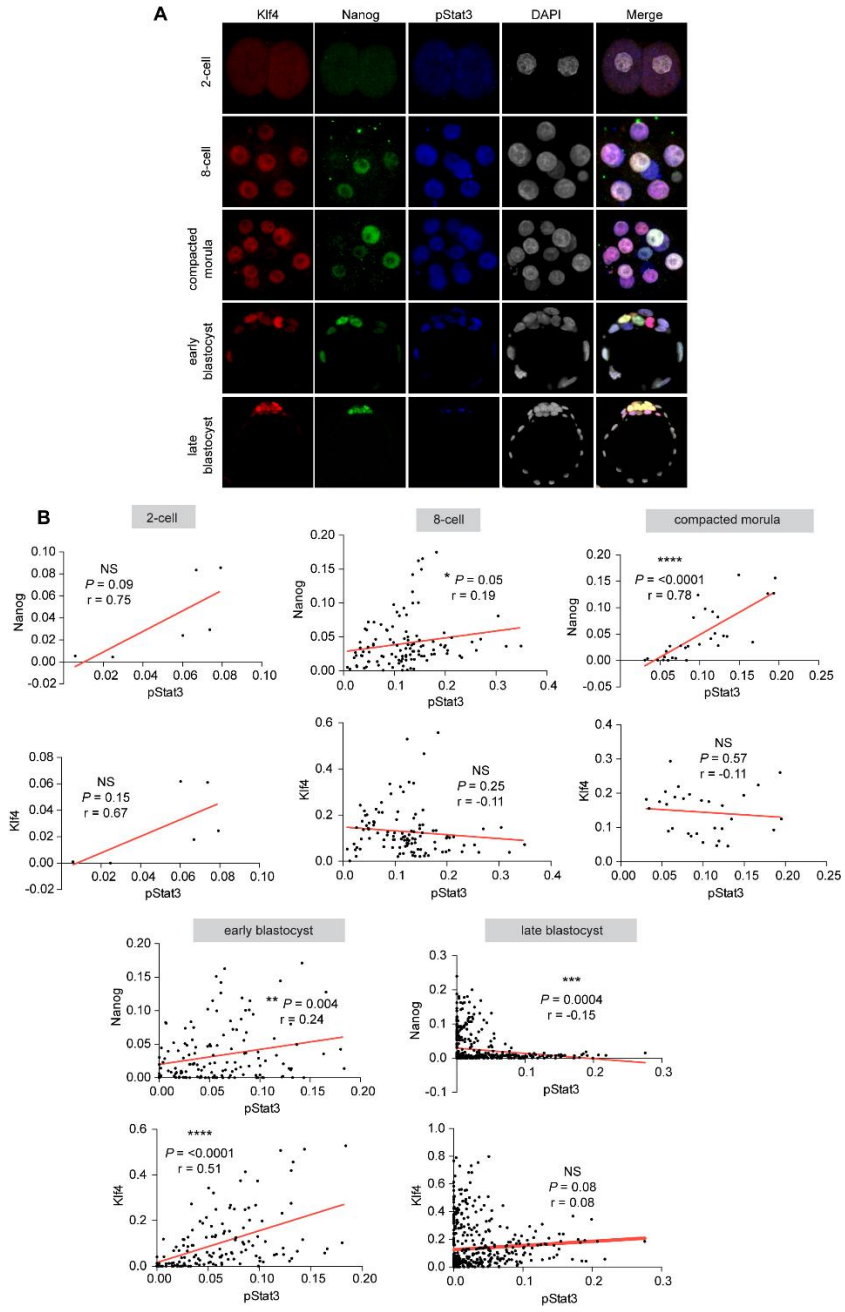

Supplementary Figure 3. Quantification of pSTAT3 and KLF4 expression during pre-implantation development. A. Immunostaining of embryos at different stages of pre-implantation development. Images from blastocyst-stage embryos represent confocal optical sections through the ICM while images of earlier stages are extended focus showing the entire embryo. **B.** Quantification of colocalisation of NANOG, pSTAT3 and KLF4 during pre-implantation development. CellProfiler was used to quantify immunostaining in individual cells. Cell nuclei were identified by manual selection and the mean pixel intensity measured in arbitrary units of intensity (a.u.). Each point represents the intensity of the noted markers within a single nucleus. Linear regression line is shown in red. *P* values indicate correlation.

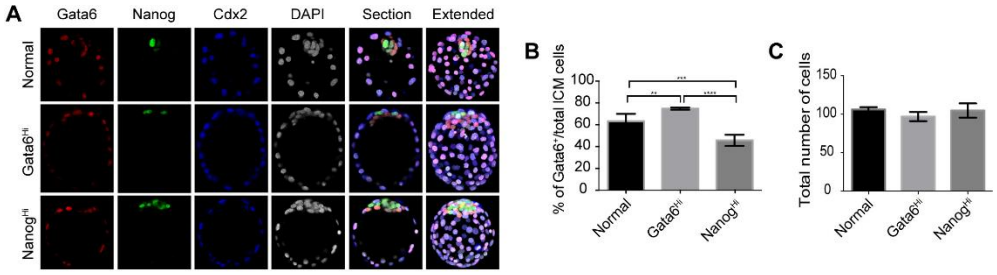

Supplementary Figure 4. Variation in PrE vs. Epi normally observed within embryo culture. Embryos were flushed from oviducts at E2.5 and cultured for 3 days in KSOM**. A.** Confocal optical sections through the ICM of late blastocysts immunostained for the 3 lineage markers, NANOG (Epi), GATA6 (PrE) and CDX2 (trophoblast) are shown for phenotype categories in control embryos. **B.** Graph displaying the % of GATA6^{+} ICM cells in each category in control (KSOM-cultured) embryos. 'GATA6^{Hi}'/'GATA6 alone' and 'NANOG^{Hi}'/'NANOG alone' embryos were pooled. ***P* = 0.0025, *** *P* = 0.0003, *****P*<0.0001, Student's unpaired t-test. **C.** Graphs displaying the total number of cells within embryos of each category. Error bars indicate average +/- s.e.m.

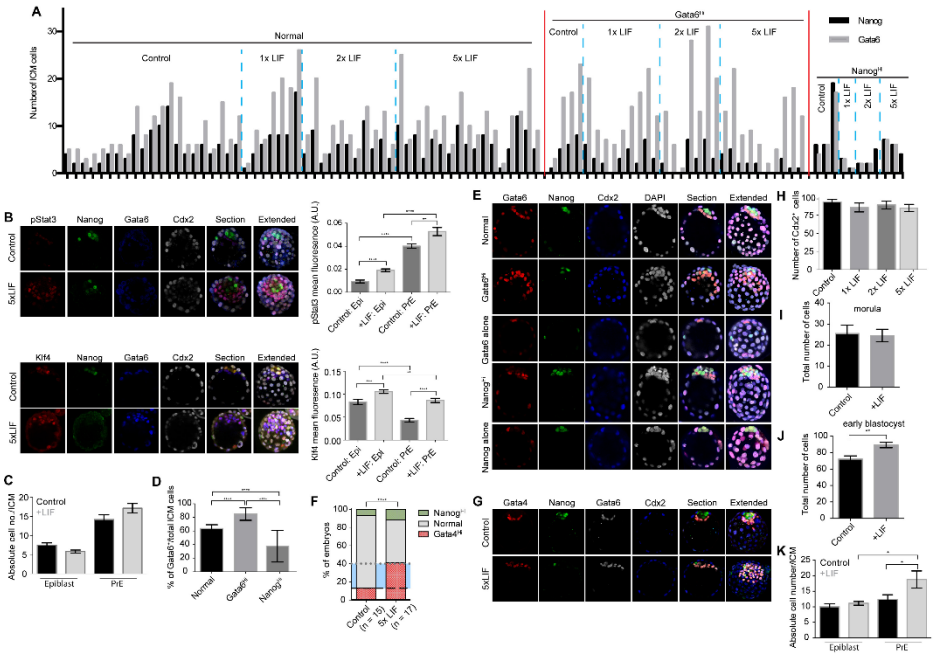

Supplementary Figure 5. LIF supports PrE cells *in vivo*. Embryos were flushed from oviducts at E2.5 and cultured for 3 days in KSOM with 5000 U (5x) LIF. **A.** Graphs displaying absolute GATA6^{+} and NANOG^{+} cell numbers in the ICM of individual embryos in 'normal', 'GATA6^{Hi}' and 'NANOG^{Hi}' embryos. Red lines divide categories and blue dotted lines divide treatments. **B.** Confocal optical sections through the ICM of late blastocysts immunostained for the 3 lineage markers, NANOG (Epi), GATA4 (PrE) and CDX2 (trophoblast) and the LIF targets pSTAT3 or KLF4. An extended focus image shows the whole embryo. Graphs show the level of pSTAT3 and KLF4 upon LIF treatment, quantified using CellProfiler (see methods). Error bars represent average +/- s.e.m. ***P* = <0.01, *** *P* = <0.001, **** *P* = <0.0001, Student's unpaired t-test **C.** Graph showing the absolute number of NANOG^{+} Epi and GATA6^{+} PrE ICM cells in embryos cultured in control conditions (KSOM) or with LIF E2.5 for 3 days. Error bars indicate average +/- s.e.m. **D.** Graph displaying the % of GATA6^{+} ICM cells in each category in LIF-treated embryos. 'GATA6^{Hi}'/'GATA6 alone' and 'NANOG^{Hi}'/'NANOG alone' embryos were pooled. ***P* = 0.0025, *** *P* = 0.0003, *****P*<0.0001, Student's unpaired t-test. **E.** Confocal optical sections through the ICM of late blastocysts immunostained for the lineage markers, NANOG (Epi), GATA6 (PrE) and CDX2 (trophoblast) are shown for phenotype categories in LIF-treated embryos. **F-G.** Embryos were flushed from

oviducts at E2.5 and cultured for 3 days in KSOM with 5000 U (5x) LIF. **F.** Graph showing categorisation of embryos immunostained for GATA4 as a marker of PrE.. The ICM of embryos was analysed based on the proportion of $GATA4^{+}$ and $NANOG^{+}$ cells. Normal embryos are those with the same proportions of PrE and Epi cells as the proportions +/- the s.d. in control (KSOM-cultured) embryos. $GATA4^{Hi}$ or $NANOG^{Hi}$ categories correspond to embryos that fell outside of the average control proportions +/- the s.d. due to having more $GATA4^{+}$ or $NANOG^{+}$ cells. The number of embryos analysed is shown below each bar. The dashed black line indicates the proportion of $GATA4^{Hi}$ embryos in control conditions. The dotted line indicates the number of embryos with high levels of GATA4. ****P<0.0001, two-tailed chi-square test. **G.** Confocal optical sections through the ICM of late blastocysts immunostained for the 3 lineage markers, NANOG (Epi), GATA4 (PrE) and CDX2 (trophoblast). An extended focus image also shows the whole embryo. **H.** Graph displaying number of $CDX2^{+}$ trophoblast cells within each condition. Error bars indicate average +/- s.e.m. **I-J.** Graph showing the total number of cells in embryos cultured in KSOM or KSOM + 5x LIF for 1 day **(I)** or 2 days **(J)**. **P = <0.01, Student's unpaired t-test. Error bars indicate average +/- s.e.m. **K.** Graph showing the absolute number of $NANOG^{+}$ Epi and $GATA6^{+}$ PrE ICM cells in embryos cultured in control conditions (KSOM) or with LIF E2.5 for 2 days. Error bars indicate average +/- s.e.m. *P = <0.05, Student's unpaired t-test.

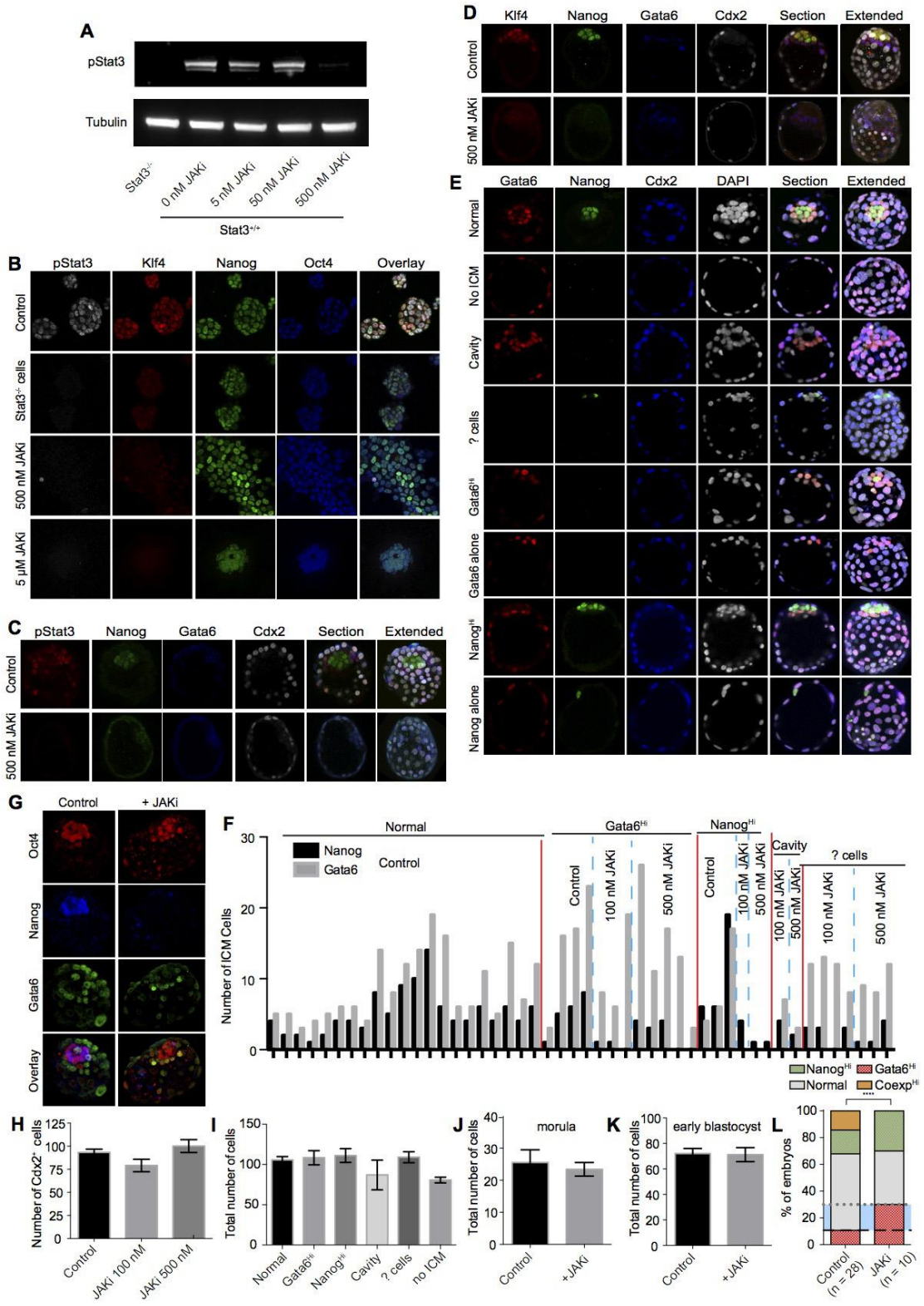

Supplementary Figure 6. JAK/STAT inhibition results in early embryonic phenotypes. A. Titration of JAKi in ESCs cultured in 2i/LIF. *Stat3*$^{-/-}$ ESCs were used as a control for the Western blot. ESCs were also cultured in 5 μM JAKi but this resulted in cell death, hence there was no sample for analysis. Tubulin levels are

shown as a loading control. **B.** Confocal optical sections through ESC colonies immunostained for pSTAT3, KLF4 and NANOG after treatment for 4 days in JAKi. *Stat3*$^{-/-}$ ESCs were used as a control for antibody specificity. At 5 μM JAKi, the majority of the ESC culture underwent cell death. A representative cluster of ESCs is shown where nuclei are enlarged and beginning to fragment. **C-E.** Embryos were flushed from oviducts at E2.5 and cultured for 3 days in KSOM alone or KSOM with 500 nM JAKi. Confocal optical sections through the ICM of late blastocysts immunostained for the 3 lineage markers, NANOG (Epi), GATA6 (PrE). CDX2 (trophoblast) and pSTAT3 **(C)** or KLF4 **(D)**. **E.** Representative embryos for the JAKi phenotype categories quantitated in Fig. 5B. '? cells' refers to embryos where cells were present within the ICM that expressed neither NANOG, GATA6 nor CDX2. **F.** Graphs displaying absolute GATA6^{+} and NANOG^{+} cell numbers in the ICM of individual embryos in 'normal', 'GATA6^{Hi}', 'NANOG^{Hi}', 'Cavity' and '? cells' embryos. Red lines divide categories and blue dotted lines divide treatments. **G.** Embryos were flushed from oviducts at E2.5 and cultured for 3 days in KSOM alone or KSOM with 500 nM JAKi. Confocal optical sections through the ICM of late blastocysts immunostained for OCT4, NANOG (Epi) and GATA6 (PrE). **H.** Graph displaying number of CDX2^{+} trophoblast cells within each condition. Error bars indicate average +/- s.e.m. **I.** Graphs displaying the total number of cells within embryos of each category. Error bars indicate average +/- s.e.m. **J-K.** Graph showing the total number of cells in embryos cultured in KSOM or KSOM + 500 nM JAKi for 1 day **(J)** or 2 days **(K)**. Error bars indicate average +/- s.e.m. **L.** Graph showing categorisation of immunostained embryos. Embryos were cultured in KSOM or KSOM + 500 nM JAKi for 2 days. The ICM of embryos was analysed based on the proportion of GATA6^{+} and NANOG^{+} cells. Normal embryos are those with the same proportions of PrE and Epi cells as the proportions +/- the s.d. in control (KSOM-cultured) embryos. GATA6^{Hi} or NANOG^{Hi} categories correspond to embryos that fell outside of the average control proportions +/- the s.d. due to having more GATA6^{+} or NANOG^{+} cells. Cells that coexpressed NANOG and GATA6 were quantified in the same manner. The number of embryos analysed is shown below each bar. The dashed black line indicates the proportion of GATA6^{Hi} embryos in control conditions. The dotted line indicates the average number of GATA6^{Hi} embryos. ****P<0.0001, two-tailed chi-square test.